

Imperial College London
Department of Electrical and Electronic Engineering
Optical and Semiconductor Devices Group

Flip-Chip Bonding using Laser Induced Ultrasonic Vibration

By

Mohd Hisham Bin Nordin

A thesis submitted in partial fulfilment for the degree of
Doctor of Philosophy

March 2016

Declaration

I herewith certify that all material in this dissertation entitled, '*Flip-chip Bonding using Laser Induced Ultrasonic Vibration*' and the work in it is my own. Other work that is not my own has been appropriately referenced and acknowledged.

Mohd Hisham Bin Nordin

Copyright Declaration

‘The copyright of this thesis rests with the author and is made available under a Creative Commons Attribution Non-Commercial No Derivatives licence. Researchers are free to copy, distribute or transmit the thesis on the condition that they attribute it, that they do not use it for commercial purposes and that they do not alter, transform or build upon it. For any reuse or redistribution, researchers must make clear to others the licence terms of this work’

Abstract

Current thermosonic flip chip bonding technologies are adversely affected by chip-to-substrate co-planarity errors and bump/pad height variations which can lead to uneven bonding strength and, in extreme cases, chip cratering. This has limited the industrial uptake of thermosonic flip chip assembly. The aim of the research reported here was to explore the use of laser-generated ultrasound as an alternative ultrasound source in flip chip bonding. The research was motivated by the idea that, with greater control over the distribution of ultrasonic energy applied over the bonding interface, it should be possible to compensate for and mitigate the above effects.

The main objective of this research work was to establish a working flip-chip bonding process using laser induced ultrasonic vibration. Initially, a literature review on current flip-chip bonding methods and laser ultrasonic methods was carried out. This suggested that confined laser ablation would be the most appropriate technique for generating strong ultrasonic vibration. Next, through modelling and simulation, an investigation was carried out to determine the suitable parameters and methods to be implemented during the experimental stage, including the pressure pulse amplitude, cavity width (irradiance spot size) and type of sacrificial material. Additional investigations were also carried out to explore the effect of applying different materials in generating ultrasonic vibration and also to show the effect of applying multiple pressure pulses simultaneously.

In the experimental phase, a custom bonding rig was developed and used to explore the parameter space for thermosonic bonding on polymer substrates using ultrasound generated by a diode-pumped solid-state laser (355 nm wavelength). Initial experiments showed unstable bond strength due to the accumulation of heat which resulted in the appearance of an unwanted glue-like substance at the bonding interface. However, this issue was overcome through careful choice of process parameters combined with the introduction of off-axis laser irradiation. A process for bonding dummy test chips to flexible substrates was successfully established, and in the best case a die shear strength of 9.3 gf/bump was achieved.

Acknowledgements

My highest appreciation goes to the Almighty God whom with His blessing and guidance are the highest reason to do whatever we would like to achieve in this worldly life.

To my supervisor, Professor Andrew S. Holmes, I would like to express my sincerest gratitude for his invaluable knowledge in guiding me throughout my PhD studies at Imperial College London. I greatly appreciate him for accepting me in the first place to be his student in the most prestigious college in the world and supporting me whenever possible.

Special thanks to the Ministry of Higher Education, Malaysia and Universiti Teknikal Malaysia Melaka (UTeM) for sponsoring me to further my study in the United Kingdom. Not to forget, Faculty of Manufacturing, UTeM and Robotics and Automation Department for continuously supporting me in furthering my studies.

I would also like to express my special thanks to many individuals and friends who have directly and indirectly involved in this study especially to my colleagues in the college, Mario, Hadri, William, Fang Jing, Tim and not forgetting Dr Munir and Susan. As well as friends in London who had helped me a lot to survive, especially Dr. Shahabuddin, Fathullah, Hadzley, Aswat, Shahrin and Wan Armizi and not to forget all of my colleagues in Malaysia.

Special thanks are dedicated to the family of Abang Manap and Kak Ana with their children Afifah, Sufyan and Safuan whom have play a major role in helping my family going through from the beginning of our live to the very end of our precious time in the great city of London. The warm welcoming and hospitality of your family will be treasured for the rest of our lives.

Deepest gratitude to my beloved parents, Dr. Nordin and Pn. Pauziah who have been my role models for my whole life and who always support me in my career. To my brothers and sister, Hazim, Nurhayati, Hafiz and Hariz, thanks a bunch for your support as well.

Deepest gratitude is also extended to my beloved parents in law, En.Murat and Pn Hasnah who have always been supportive in my studies. To my in-laws, Azraai, Izzar and Illani, thank you too for your priceless support.

Finally, infinite of thanks and loves to my very understanding and supportive beloved wife, Izuan Murat and our children, Izzahin, Irissafina and Izzafri for their loves and patience throughout this studies. Without them none of this would have been possible.

Table of Contents

Declaration	2
Copyright Declaration	3
Abstract	4
Acknowledgements	5
Table of Contents	6
List of Figures	9
List of Tables	13
1. INTRODUCTION	14
1.1 Background	14
1.2 Problem statement and research motivation	14
1.3 Research objective and thesis outline	17
2. LITERATURE REVIEW	18
2.1 Thermosonic flip-chip bonding.....	18
2.2 Laser ultrasonic bonding.....	22
2.3 Laser ablation.....	26
2.3.1 Generation of pressure pulse induced by laser ablation	26
2.3.2 Pressure versus displacement	29
2.3.3 Confined ablation	29
2.3.4 Pressure propagation	36
2.3.5 Thermal characteristics.....	39
2.4 Ultrasonic vibration detection methods	42
3. MODELLING AND SIMULATION	44
3.1 System set-up	44
3.2 Boundary settings for pressure acoustic and plane stress modules.....	46
3.3 Simulation results and discussion	51
3.4 Tests, modifications and further simulation results	56
3.4.1 Varying pressure pulse magnitude	56
3.4.2 Optimising pressure pulse cavity size	59
3.4.3 Effect of applying pressure pulse to all target simultaneously	65
3.4.4 Changing sacrificial material.....	67
3.3 Summary	72

4. LASER ULTRASONIC BONDING SYSTEM	73
4.1 System overview	73
4.2 System architecture	74
4.2.1 Thermosonic bonder	76
4.2.2 Laser system	77
4.2.3 Precision XYZ stage	78
4.2.4 Temperature Controller	81
4.2.5 Bond force control	83
4.3 Process flow	85
4.3.1 Sample preparation	85
4.3.2 Heating	86
4.3.3 Laser setup, calibration and laser path alignment	87
4.3.4 Irradiation	91
4.3.5 Evaluation	93
4.4 Evaluating electrical connectivity	94
4.5 Evaluating bonding strength	96
4.6 Summary	99
5. EXPERIMENTAL INVESTIGATION OF LASER ULTRASONIC FLIP-CHIP BONDING.....	100
5.1 Experimental design	100
5.1.1 Initial parameters for laser thermosonic bonding process	103
5.1.2 Experimental process flow	105
5.1.3 Justification on using continuous improvement method	107
5.2 Establishing laser thermosonic flip-chip bonding process	108
5.3 Bond strength improvement through modifications	113
5.4 Failure modes	123
5.5 Damage analyses on TSFC bonding using laser ultrasonic vibration	124
5.6 Summary	126
6. CONCLUSIONS AND FUTURE WORK	127
6.1 Summary of achievement	127
6.2 Suggestions for future work	128
6.3 Contributions	129

References	130
APPENDIX A - Model Validation using COMSOL Multiphysics.....	134
APPENDIX B - Effects of varying dimensions of chip and structure to the resulting displacement.....	135
APPENDIX C – Bipolar Effect Modelling	136
APPENDIX D – Varying Cavity Width.....	137
APPENDIX E - Vibration Effect on Nearby Interconnects.....	140
APPENDIX F – Relationship between diode current and laser power.....	143
APPENDIX G – Off-axis modelling of pressure induced vibration.....	144

List of Figures

1.1	A possible scheme for laser ultrasonic flip-chip bonding, with ultrasonic generation in a carrier tape	15
1.2	Laser assisted bumping process (from [6])	16
2.1	Thermosonic bonding tools, showing (a) longitudinal and (b) transverse geometries (from[8])	19
2.2	Typical vibration amplitude of tool and chip during bonding process (from[4])	20
2.3	(a) Tool and chip vibration amplitude at the bonding forming stage. (b) Tool and chip vibration amplitude at the bonding increase stage. (from [4])	20
2.4	Longitudinal bonding (from[10])	21
2.5	Displacement of the surface layer opposite the ablation spot for PS sample (from [16])	24
2.6	Displacement of the surface layer opposite the ablation spot for a PMMA sample (from [16])	25
2.7	Graph of Radiant Exposure versus Peak Stress (from [15])	27
2.8	Peak amplitude of the stress wave as a function of fluence for polyimide film irradiated with the 308 nm and 193 nm lasers (from [23])	27
2.9	Peak stress as a function of fluence for (a) femtosecond laser and (b) nanosecond laser (from [27])	28
2.10	Direct ablation (from [29])	31
2.11	Confined ablation (from [29])	31
2.12	Dependence of the coupling coefficient on the laser intensity for the direct ablation, confined ablation and confined ablation with vacuum grease on the target layer interface of a 2mm thick aluminium irradiated with 7ns (532 nm wavelength) (from [20])	32
2.13	Graph of gap width versus coupling coefficient (from [30])	32
2.14	Dependence of coupling coefficient on laser energy for 1mm diameter cavity (open squares), 2mm diameter cavity (open circles) and planar target (closed circles) (from [31])	33
2.15	Effect of cover layer thickness on coupling coefficient for different laser intensities (from [31])	34
2.16	Maximum pressure versus thickness for copper and aluminium foils (from [32])	35
2.17	Laser generation of ultrasound in (a) thermoelastic regime and (b) ablation regime (from [34])	36
2.18	Typical shape of acoustic pulse generated in polyimide by xenon–chloride (XeCl, 308 nm) excimer laser ablation with long pulse duration of 100 ns.(from [35])	37
2.19	Transducer signal generated by irradiation at 308 nm of 125 μm thick polyimide for radiant exposures of 34 (top) and 18 mJ/cm^2 (bottom) (from [15])	37
2.20	Bipolar stress wave (from [36])	38
2.21	Unipolar stress wave (from [36])	38
2.22	Temperature profiles for polyimide ablation at a) 1 kHz and b) 10 kHz(from [37])	40
2.23	Depth profile of temperature in polyimide (PI) 10 μs to 1 s after irradiation with a 10 μJ pulse (20 μm spot size diameter) at 355 nm wavelength (from [38])	41
2.24	Simulated surface profile for multiple 10 μJ laser pulses (from [38])	41

2.25	Laser drilled holes ranging from 1 shot to 30 shots (from [38])	42
2.26	Measuring vibration using out-plane and in-plane vibrometers (from[8])	43
3.1	Basic structure used in modelling	45
3.2	Boundary settings for pressure acoustics	47
3.3	Pressure source profile	47
3.4	Boundary settings for plane stress	48
3.5	Solver parameters	49
3.6	Free mesh parameters setup using extra fine predefined mesh size	50
3.7	Generated mesh for extra fine predefined mesh size	50
3.8	Pressure versus time graph for 100 MPa pressure pulse	52
3.9	Pressure probe points	52
3.10	Displacement probe point	53
3.11	Displacement versus time graph for 100 MPa pressure pulse at probe point in Figure 3.10	54
3.12	Displacement versus time graph at bonding interface for a 100 MPa pressure pulse, over a time interval of 0.5 μ s	55
3.13	Pressure versus time graph for 500 MPa pressure pulse at probe points in Figure 3.9	57
3.14	Displacement versus time graph at bonding interface for a 500 MPa pressure pulse	57
3.15	Graph of applied pressure versus resulting pressure at bonding interface	58
3.16	Graph of applied pressure versus vibration amplitude at bonding interface	59
3.17	Displacement probe points for nearby interconnects	61
3.18	Cavity depth at 35 μ m	63
3.19	Displacements at all interconnect sites for a 35 μ m cavity depth, based on probe points in Figure 3.17	63
3.20	Displacements at all interconnect sites for a 70 μ m cavity depth, based on probe points in Figure 3.17	64
3.21	Model with 5 cavities	65
3.22	Vibration characteristics with multiple pressure pulses applied simultaneously	66
3.23	Vibration characteristic for aluminium as a sacrificial material	67
3.24	Pressure attenuation for (a) aluminium and (b) polyimide	68
3.25	Vibration characteristic for (a) gold and (b) copper as a sacrificial material	69
3.26	Pressure attenuation for (a) gold and (b) copper	70
3.27	Graph of acoustic impedance versus displacement	71
3.28	Graph of acoustic impedance versus attenuated pressure	71
4.1	a) chip and b) flex substrate (with enlargement images)	73
4.2	Schematic of custom-built TS bonder for laser ultrasonic application	74
4.3	Thermosonic bonding system block diagram	75
4.4	Custom-built TS bonder a) complete assembly, b) simplified assembly, c) tilt stage	76
4.5	Laser system block diagram	77

4.6	ASI PZ2000 XYZ stage	78
4.7	ASI XYZ stage main window	79
4.8	ASI XYZ joysticks	80
4.9	ASI XY pad	80
4.10	a) CAL 9900 series temperature controller b) PT100 temperature sensor c) heater rods	81
4.11	Temperature sensor and heater rods configuration	82
4.12	Hot stage temperature control system diagram	82
4.13	TS bonder heating rate	83
4.14	Flexible force sensor	84
4.15	Graph of bond force versus output resistance	84
4.16	Laser ultrasonic bonding overall process flow	85
4.17	a) Evenly clamped sample b) Uneven clamped sample	86
4.18	Slight misalignment of a clamped sample	87
4.19	Rotated laser path for 88 misaligned interconnects	88
4.20	Spectra-Physics controller interface	89
4.21	Targeting position for laser irradiation spot	90
4.22	Manual laser control interface	90
4.23	Distance from minimum focal plane versus ablated spot diameter	92
4.24	Specially designed electrical connections schematic for $4w\Omega$ joint resistance measurement in a TS assembly (from [43])	94
4.25	Keithley 2000 Multimeter	94
4.26	Four-wire probe station with Keithley 2000 multimeter	95
4.27	Probing 4 traces on a bonded flip-chip and flex substrate	95
4.28	Manual shearing device and its schematic diagram	96
4.29	Calibration schematic diagram for manual shearing device	97
4.30	Compressive force (g) versus spring displacement (mm) graph	98
5.1	Pitch distance between two adjacent bumps (pitch size) and laser beam spot	102
5.2	First stage experimental flow chart	106
5.3	Glue like residue on chip surface	109
5.4	Melted inner surface of UV glass	110
5.5	Damaged substrate layer and its close up view	112
5.6	Full penetration of the sacrificial PI layer and its close up view	112
5.7	Plasma damages on glass layer at the ablation interface	112
5.8	Double-substrate configuration	114
5.9	Exposed metallic pads on flex sacrificial layer	115
5.10	a) normal ablation depth b) ablation depth with angle of incidence	116
5.11	Ablation depths for a) normal ablation b) ablation with 20° laser incidence	116
5.12	Introduction of laser incidence angle by physical tilting of TS bonder	117
5.13	Minor traces of glue like substance and enlarged bonding sites	118

5.14	Test positions on chip with respect to image in Figure 5.13	118
5.15	Variation in laser beam diameter with 30° work piece tilt angle	119
5.16	Chip from second tilted test, with slight traces of glue-like substance	121
5.17	Successful bonding with improved handling method	122
5.18	Completely torn off bump adhered firmly to the substrate pad	123
5.19	Ablated PI layer a) top view b) bottom view	124
5.20	Damages on confinement glass	125
5.21	Close up view of holes produced in confinement glass a) 10x magnification b) 50x magnification	125
7.1	Configuration and plane stress modelling setting for work in [16] and [19]	134
7.2	Resulting displacement at probe point in Figure 7.1	134
7.3	Modified modelling structure from Figure 3.9	136
7.4	Resulting compression, rarefaction and reflection in propagating wave at probe point in Figure 7.3	136
7.5	Vibration at 20 µm cavity width	137
7.6	Vibration at 40 µm cavity width	137
7.7	Vibration at 60 µm cavity width	138
7.8	Vibration at 80 µm cavity width	138
7.9	Vibration at 100 µm cavity width	139
7.10	Vibration at 120 µm cavity width	139
7.11	Multiple vibrations at 20 µm cavity width	140
7.12	Multiple vibrations at 40 µm cavity width	140
7.13	Multiple vibrations at 60 µm cavity width	141
7.14	Multiple vibrations at 80 µm cavity width	141
7.15	Multiple vibrations at 100 µm cavity width	142
7.16	Multiple vibrations at 120 µm cavity width	142
7.17	Graph of laser power versus frequency for various diode currents for Talon® 355-15 UV diode-pump solid state (DPSS) Q-switched laser	143
7.18	30 degrees angle of incidence (initial)	144
7.19	x-axis (0.15 µm)	144
7.20	y-axis (0.1 µm)	144
7.21	30 degrees angle of incidence (final)	145
7.22	x-axis (0.17 µm)	145
7.23	y-axis (0.13 µm)	145

List of Tables

2.1	TSFC Bonding Parameters (from [4])	19
2.2	Breakdown threshold for fused silica as a function of laser pulse duration at a wavelength of 1.06 μm (from [33])	35
3.1	Material dimensions and properties	46
3.2	Resulting y-displacement with respect to cavity width	60
3.3	Resulting y-displacement for all bumps with respect to cavity width	61
3.4	Resulting y-displacement for all bumps with respect to cavity depth at 80 μm cavity width	64
3.5	Attenuated pressures for different materials	71
3.6	Initial parameters for experimental works	72
4.1	Laser parameters	91
5.1	Parameter limits and working ranges	101
5.2	Initial laser thermosonic bonding parameters	103
5.3	Data for determining maximum bonding time	104
5.4	Parameters matrix	107
5.5	Repetitive bonding trial results	111
5.6	Double-substrate tests	114
5.7	$4w\Omega$ measurement result for 30° laser incidence angle	117
5.8	$4w\Omega$ measurement result for 30° laser incidence angle (2 nd Test)	120
5.9	$4w\Omega$ measurement result for 30° laser incidence angle (3 rd Test)	122
5.10	Failure joint	123
5.11	Process parameters for successful bonding	126
7.1	Varying chip thickness with constant width at 100 MPa (100 μm cavity width)	135
7.2	Varying chip width with constant thickness at 100 MPa (100 μm cavity width)	135

1. INTRODUCTION

1.1 Background

Ultrasonic bonding is recognised as one of the effective joining methodologies in flip-chip assembly for microelectronics. It is attractive because it allows bonding at relatively low temperatures (typically 200 °C) and leads to direct metal-metal bonds without the need for additional materials. It also provides strong metallurgical joining [1] which is expected to be more reliable than solder interconnection and conductive adhesive [2], [3].

The most widely adopted ultrasonic bonding method currently is thermosonic bonding. This technique uses a transducer powered by a piezoelectric element to transmit ultrasonic vibration to the bonding interface. In the case of flip-chip assembly this interface is the boundary between the “bumps” (metallised contact pads) on the flip-chip and the substrate pads. The ultrasonic vibration, together with sufficient clamping force, will cause the initiation of a bond in about 7.5 ms [4]. The basic principle of thermosonic bonding is the introduction of an ultrasonic softening effect at the bonding interface that allows the materials to undergo plastic deformation. During the plastic deformation, oxides and contaminations are removed from the contact surfaces of connecting materials, exposing raw surface which enables the materials to bond [5] on a typical timescale of tens of milliseconds. This ultrasonic energy, coupled with external force, also does not require or generate high temperature that can damage sensitive chips or substrates.

1.2 Problem statement and research motivation

Thermosonic bonding is classified as either transverse or longitudinal depending on whether the ultrasonic vibration lies parallel to or perpendicular to the bonding interface. In both cases, the ultrasonic energy is introduced via the bonding tool and is therefore coupled to the entire chip. This can cause irregularity in the bonding energy distributed to individual bumps, especially if the chip is large and/or the bumps are not symmetrically disposed on the chip surface. As a result, the bonding strength may vary from bump to bump and this can lead to increased incidence of electrical connectivity failures, which will surely affect the overall device functionality. Slight variations in bump height across the chip can also lead to bond strength variations.

One possible way to improve bond strength uniformity is to use a bonding method that can channel a controlled amount of ultrasonic energy individually to each bump. The normal thermosonic bonding process cannot achieve this because it relies on coupling of the ultrasonic energy from the bond tool to the entire chip.

Therefore, the motivation of the present work was to explore the possibility of using pulsed laser light to generate ultrasonic excitation in a more targeted manner. There is a higher chance of establishing flip-chip bonding using the vibration induced by laser at micro scale if the vibration characteristics can be imitated from current thermosonic flip-chip bonding process. In addition, with greater control over the distribution of ultrasonic energy applied over the bonding interface, it should be possible to compensate for and mitigate the uneven bonding strength and chip cratering effects.

Figure 1.1 shows how this approach might be applied in practice to flip-chip assembly. In this particular implementation, the substrate is held on a polymer carrier tape which also acts as an absorber for the laser light. The light is incident through the (transparent) bond head, and generates an ultrasonic wave either through thermoelastic expansion or ablation at the top surface of the tape. Depending on the size and shape of the laser beam, the ultrasonic excitation can be more or less localised, allowing for the possibility of either parallel bonding of many I/Os, or sequential bonding at individual I/O sites.

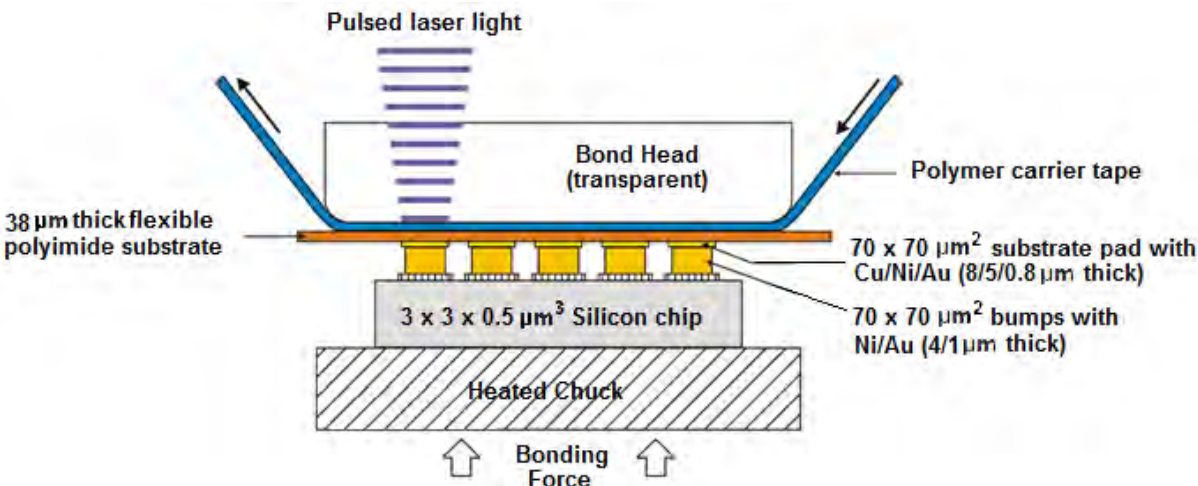


Figure 1.1 A possible scheme for laser ultrasonic flip-chip bonding, with ultrasonic generation in a carrier tape

Laser technology has been used previously in flip-chip assembly as part of a process for transferring metal bumps onto flip chips [6]. This so-called “laser assisted bumping” process involves three steps, (see Figure 1.2):

- 1) fabrication of bumps on a carrier;
- 2) bonding of the bumps to a chip using a conventional thermosonic bonder;
- 3) release of the bumps from the carrier by laser machining of a sacrificial polyimide layer.

The proposed laser ultrasonic bonding technique could potentially replace the conventional thermosonic bonding step in this process. It may even be possible to combine the bonding and release operations, making the whole process simpler and faster to implement.

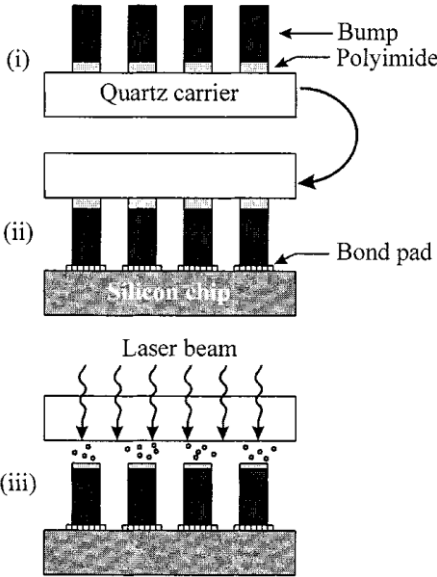


Figure 1.2 Laser assisted bumping process (from [6])

1.3 Research objectives and thesis outline

The overall purpose of this research is to establish the feasibility of flip-chip bonding using laser induced ultrasonic vibration. Initially, the objective is to establish a flip-chip bonding by a mere adherence of a dummy flip chip to a flex substrate, which is sufficient to prove the hypothesis. Then, through modifications of the process or experimental setup, the bond strength (die shear strength) of the adhered flip-chip to the flex substrate should exceed the minimum standard for die shear stress test.

In order to achieve this objectives, several steps have been taken which include reviewing current methodologies and related topics, modelling and simulation and conducting experiments. The remainder of this thesis is organised as follows. Chapter 2 reviews current thermosonic flip-chip bonding processes, identifying the important parameters to be studied, as well as important topics such as ultrasonic vibration and laser generation of ultrasound. Modelling and simulating of a flip-chip structure for the new laser-generated ultrasound method is presented in Chapter 3. Through the modelling and simulation work, the acoustic vibration characteristics at the point of interests were studied and important parameters for the initial setup of the experimental work were determined.

Based on the work described in the preceding chapters, Chapter 4 presents the system set up and processes for the flip-chip bonding using the laser-generated ultrasound method, while Chapter 5 presents the experimental results and some modifications to the process. The final chapter concludes the finding and contribution of this research and suggests future works that can be done to improve this method.

2. LITERATURE REVIEW

In order to develop a laser ultrasonic approach to flip-chip bonding, a wide range of knowledge is required. This chapter contains a review of current thermosonic flip-chip bonding processes, laser generation of ultrasound, confined laser ablation, pressure propagation in multilayer structures and ultrasonic vibration detection methods.

2.1 Thermosonic flip-chip bonding

Thermosonic flip-chip bonding is a solderless technology for area-array connections [7]. It is similar to thermocompression bonding in terms of simplicity and in being a clean, solderless solid-state bonding approach, but requires much lower pressure, temperature and bonding time as a result of introducing ultrasonic energy into the process [8]. Basically, thermosonic flip-chip (TSFC) bonding is an adaptation of wire bonding technology for flip-chip assembly. Instead of joining one connection at a time (either wire to chip or wire to carrier/substrate), TSFC is able to form hundreds of joints simultaneously between a chip and a substrate or carrier. As with the wire bonding process, heat, ultrasonic energy and pressure are combined to form solid state metal-metal bonds [9]. However, TSFC has higher electrical performance when compared to wire bonding due to the fact that it has shorter interconnect distance between chip and board. The high input / output (I/O) density of this bonding system also enables miniaturization of products, which is more desirable to microelectronic packaging industries [6].

A TSFC system is normally classified as being either transverse or longitudinal according to the direction of ultrasonic vibration transmitted by the bonding tool [8]. In both transverse and longitudinal bonding systems, ultrasonic vibration, which is generated by a transducer, is transmitted to the chip through a bonding tool, also referred as a collet (Figure 2.1). Basically, a transducer for thermosonic bonding consists of a piezoelectric element, which is the source of the ultrasonic vibration, an amplifying horn and a collet. The collet in the transverse bonding system is fixed perpendicular at the horn tip, while in the longitudinal bonding system the collet is fastened axially with the horn [8]. Both systems operate by holding the chip firmly using vacuum suction through the collet which is hollow in structure.

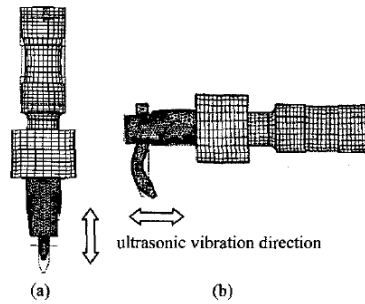


Figure 2.1 Thermosonic bonding tools, showing (a) longitudinal and (b) transverse geometries (from [8])

To develop a new bonding system for flip-chip assembly, it is essential to identify the important parameters involved in establishing successful bonding in TSFC. The important parameters to be studied that could determine the quality of successful bonding are the ultrasonic power, ultrasonic frequency, bonding force (the static normal pre-load applied at the interface), bonding time and substrate temperature [4]. The parameters associated with ultrasonic vibration are the frequency and amplitude of the bonding tool and chip, which are driven by the ultrasonic generator. From experimental works using a transverse bonding system with bonding parameters set as in Table 2.1, a normal TSFC bonder starts to form a bond after about 7.5 milliseconds. At this stage, a stick and slide motion of the chip is expected to occur until it finally stabilize slightly before 10 milliseconds of the bonding duration. Once bonding has been initiated, the remaining time is used to strengthen the bond. It can be observed that during the bonding increase stage (Figure 2.2), the amplitude of the chip vibration is about 1 μm which is adequate for successful bonding.

Table 2.1 TSFC Bonding Parameters (from [4])

I/O count	8 bumps
Bonding force	30 g/bump
Substrate temperature	163 °C
Ultrasonic frequency	56 kHz
Ultrasonic power	2-3 W
Bonding time	22.5 ms

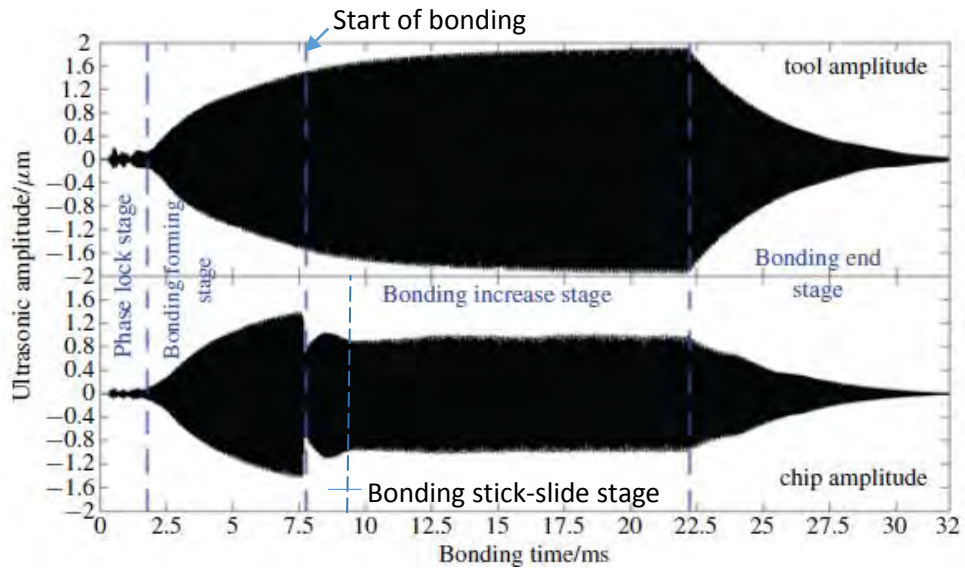


Figure 2.2 Typical vibration amplitude of tool and chip during bonding process (from [4])

During the bonding increase stage, it is observed that the bonding tool does not move simultaneously with the chip as shown in Figure 2.3b as can be compared from the vibration profile of the tool and chip at the beginning of the bonding process shown in Figure 2.3a. As a result, ultrasonic energy is wasted as only part of the ultrasonic energy has been propagated to chip. In addition, silicon cratering has been observed which is caused by the relative movement between tool and chip [4].

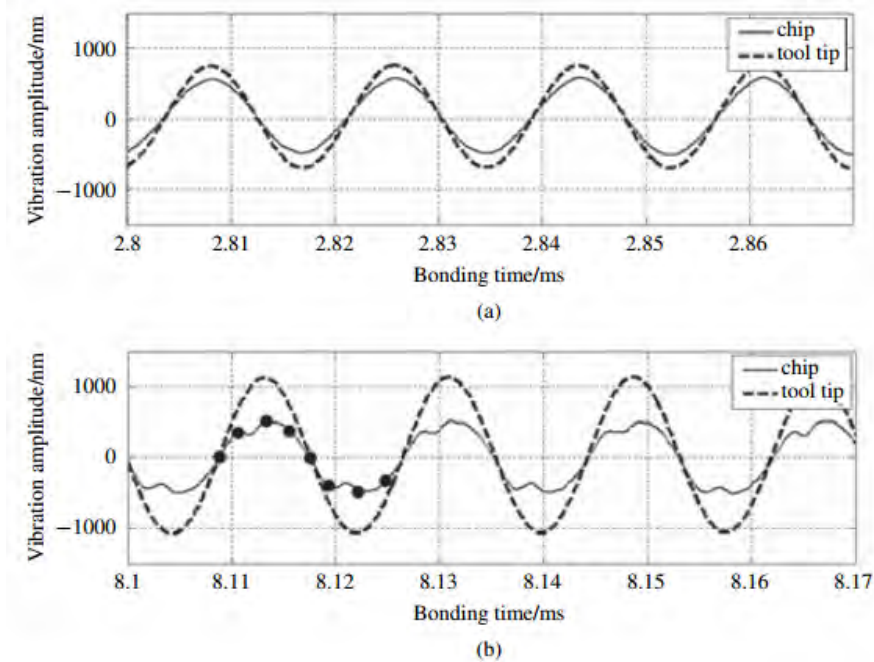


Figure 2.3 (a) Tool and chip vibration amplitude at the bonding forming stage. (b) Tool and chip vibration amplitude at the bonding increase stage. (from [4])

One of the major problems associated with transverse flip-chip bonding systems is the planarity issue which is caused by improper alignment between tool and chip. This improper alignment will lead to a non-uniform pressure being applied across the chip resulting in over-bonding at the bumps with higher compressive stress and under-bonding at the bumps with lower stress [8]. This effect becomes more severe for high I/O assemblies since the bonding force, which is proportional to the number of I/Os, increases. The planarity issue is also believed to be caused by the bending of the collet attached to the bonding tool in the transverse motion when high bond force is applied [8]. To overcome this problem, the longitudinal bonding approach has been studied [10]. In a longitudinal bonding system, the bonding force and ultrasonic vibration are aligned and also parallel with the horn of the bonding tool, as illustrated in Figure 2.4. From simulation and experiments [8], it has been shown that for longitudinal bonding, even under high loading, the collet can maintain adequate co-planarity between the chip and the substrate.

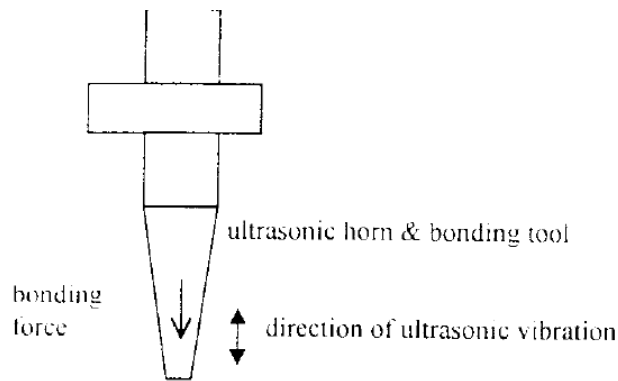


Figure 2.4 Longitudinal bonding (from [10])

Unfortunately, longitudinal bonding generates higher stress levels at the bonding interface than transverse bonding. For example, the ultrasonic hammering impact generated by a longitudinal bonding system with an ultrasonic power of 2 W may reach 1.2 GPa at a bonding force of 200 gf per bump, which is 20% higher than for the transverse mode [8]. This explains why, in reference [8], chip cratering was observed in the longitudinal mode while no cratering was observed in the transverse mode. Furthermore, while it has been argued that longitudinal bonding can be used for high I/O assembly, it is agreed that it requires higher bonding force. This is not an issue for the longitudinal bonder [10]. However the higher force increases the likelihood of cratering on the silicon chip. Therefore, longitudinal bonding has not been widely adopted for flip-chip assembly in high I/O applications even though it solves the chip tilting issue.

2.2 Laser ultrasonic bonding

One of the main motivations for exploring the proposed laser ultrasonic bonding approach is the possibility of applying ultrasonic energy in a controllable manner to localised regions of the chip. With this capability it should be possible to adjust the applied ultrasonic energy to compensate for variations in the bonding force. Even in the absence of co-planarity errors, bonding force variations can arise from non-uniform bump height or substrate distortions. With compensation of this type in place, it should be possible to reduce the overall bonding force, and hence lower the likelihood of cratering. This assumes that it is possible to measure or predict the bonding force variations, but there are optical metrology techniques that could do this.

Conventional thermosonic bonding operates on the principle of ultrasonic or acoustic softening which is defined as “the decrease in the plastic (yield) limit of a material under intense ultrasonic vibration” [11]. It is assumed that the proposed laser ultrasonic bonding process will work on the same principle. However, the ultrasonic generation mechanism will be quite different, being based on thermoelastic material expansion or ablation rather than piezoelectric effect. One consequence of this is that, depending on the laser type used, a wide range of vibration frequencies will be available. In contrast, conventional thermosonic bonders use only a small number of standard frequencies, with many operating at 60 kHz.

Equation (2.1) is used to calculate the acoustic energy density [12] as follow:

$$E = \xi^2 \omega^2 \rho \quad (2.1)$$

Where E = acoustic energy density

ξ = vibration amplitude

ω = excitation angular frequency

ρ = density

Since the laser-induced ultrasonic vibration works basically on the same principle, this equation can also be used to determine its acoustic energy. By assuming that the acoustic energy density required in the laser process will be same as for conventional TSFC, the amplitude and frequency in Equation (2.1) can be adjusted accordingly to give similar result (depending on the limit of each parameter). For example, if the vibration amplitudes generated by laser are small, the laser process can be compensated by increasing the ultrasonic frequency.

The identified laser ultrasonic parameters that might affect the ultrasonic vibration amplitude and frequency are the laser peak power, laser spot size (area), laser pulse duration, type of target material (speed of sound) and material thickness. Depending on the laser irradiation mode, other material properties are also important such as optical absorption at laser wavelength, thermal conductivity and heat capacity (if thermoelastic mode is used) and ablation characteristics (if ablation mode is used). These parameters will be investigated to characterize the laser ultrasonic requirement for flip-chip bonding.

There are potentially two methods for generating laser ultrasonic vibration which are by thermoelastic expansion or by ablation. The thermoelastic expansion process is widely used in non-destructive inspection of materials or objects [13] due to its nature which doesn't produce any damage to the material surface, while ablation is known to be used in material removal processes such as laser machining [14].

It is quite desirable to implement the thermoelastic concept in generating ultrasonic vibration as the means for ultrasonic bonding since the process is much simpler than the ablation process. However, the vibration amplitude produced by the thermoelastic effect is relatively low compared to that produced by ablation. Theoretically, the amplitude generated by thermoelastic expansion of a polyimide at an acoustic pressure of 1 MPa [15] (normal peak stress generated during thermoelastic expansion) will only be about 8.6 nm at 10 MHz (calculated from pressure pulse duration of 100ns). These values are calculated by using the acoustic pressure formula as in Equation (2.2) where $\rho = 1430 \text{ kg.m}^{-3}$ and $c = 1300 \text{ m.s}^{-1}$.

$$P = \rho c \omega \xi \quad (2.2)$$

Where $P = \text{acoustic pressure}$

$\rho = \text{density}$

$c = \text{speed of sound}$

$\omega = \text{excitation angular frequency}$

$\xi = \text{vibration amplitude}$

Other possible materials such as copper and aluminium also produce very low displacement amplitude. For example, using the same values for pressure and excitation angular frequency, these materials give displacements of 0.47 nm and 1.2 nm respectively. With such small displacements it is not possible to generate enough ultrasonic energy density for bonding. For comparison, using Equation (2.1) to determine the ultrasonic energy required (silicon chip),

normal thermosonic bonding generates 331 J/m^3 of energy density at 60 kHz (displacement = $1 \text{ }\mu\text{m}$), whereas the ultrasonic energy density generated by thermoelastic expansion of silicon at 10 MHz (displacement = 0.8 nm) is only 5.88 J/m^3 .

On the other hand, the ablation method has the potential to be exploited as it is possible to generate higher amplitudes up to few micrometres [16]. Although it is often used for material removal in applications such as fine material cutting, etching and submicrometer patterning [15], it is also possible to utilize this technique for more exotic applications such as vibration generation. There are many research publications in the area of non-destructive testing that demonstrate the presence of laser-induced ultrasonic vibration (see for example [17], [18]). Unfortunately the resulting amplitude of the generated vibration is either too small or the frequency is too low to be useful in the present work.

One investigation of vibrations induced by ablation is discussed in [16]. In this research, the materials investigated were polystyrene (PS) and polymethylmethacrylate (PMMA) of a thickness ranging from $20\text{-}100 \text{ }\mu\text{m}$. The laser used in the ablation process was a KrF excimer laser ($\lambda = 248 \text{ nm}$) and the waves were detected using a Laser Doppler Vibrometer (LDV) at the opposite side of the test materials. The measured displacements are shown in Figures 2.5 and 2.6.

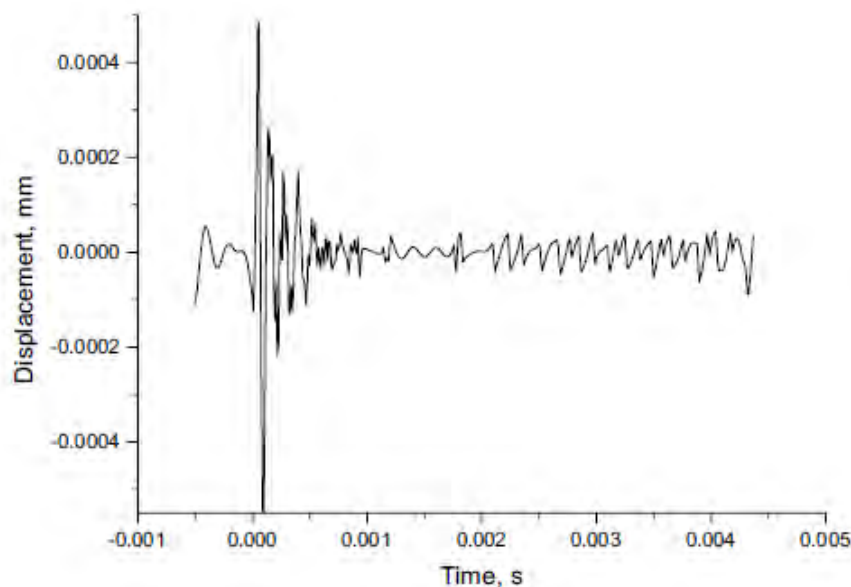


Figure 2.5 Displacement of the surface layer opposite the ablation spot for a PS sample (from [16])